5-15-2009

Coupling of Integrated Biosphere Simulator to Regional Climate Model Version 3

Jonathan M. Winter
Massachusetts Institute of Technology

Jeremy S. Pal
Loyola Marymount University, jpal@lmu.edu

Elfatih A. B. Eltahir
Massachusetts Institute of Technology

Coupling of Integrated Biosphere Simulator to Regional Climate Model Version 3

JONATHAN M. WINTER

Massachusetts Institute of Technology, Cambridge, Massachusetts

JEREMY S. PAL

Loyola Marymount University, Los Angeles, California

ELFATIH A. B. ELTAHIR

Massachusetts Institute of Technology, Cambridge, Massachusetts

(Manuscript received 19 March 2008, in final form 4 September 2008)

ABSTRACT

A description of the coupling of Integrated Biosphere Simulator (IBIS) to Regional Climate Model version 3 (RegCM3) is presented. IBIS introduces several key advantages to RegCM3, most notably vegetation dynamics, the coexistence of multiple plant functional types in the same grid cell, more sophisticated plant phenology, plant competition, explicit modeling of soil/plant biogeochemistry, and additional soil and snow layers.

A single subroutine was created that allows RegCM3 to use IBIS for surface physics calculations. A revised initialization scheme was implemented for RegCM3–IBIS, including an IBIS-specific prescription of vegetation and soil properties.

To illustrate the relative strengths and weaknesses of RegCM3–IBIS, one 4-yr numerical experiment was completed to assess ability of both RegCM3–IBIS (with static vegetation) and RegCM3 with its native land surface model, Biosphere–Atmosphere Transfer Scheme 1e (RegCM3–BATS1e), to simulate the energy and water budgets. Each model was evaluated using the NASA Surface Radiation Budget, FLUXNET micrometeorological tower observations, and Climate Research Unit Time Series 2.0. RegCM3–IBIS and RegCM3–BATS1e simulate excess shortwave radiation incident and absorbed at the surface, especially during the summer months. RegCM3–IBIS limits evapotranspiration, which allows for the correct estimation of latent heat flux, but increases surface temperature, sensible heat flux, and net longwave radiation. RegCM3–BATS1e better simulates temperature, net longwave radiation, and sensible heat flux, but systematically overestimates latent heat flux. This objective comparison of two different land surface models will help guide future adjustments to surface physics schemes within RegCM3.

1. Introduction

In January 1981, the *New York Times* article ''Down on the farm, higher prices'' (King 1981) explained the economic impacts of drought, predicting a 10%–15% increase in average U.S. consumer food bills resulting from a lack of rainfall in 1980. Agricultural productivity is strongly correlated to soil moisture, as examined by studies such as that of Claassen and Shaw (1970). As the world's food supply continues to be taxed by burgeoning populations, a greater percentage of arable land will need to be utilized and land currently producing food must become more efficient.

The need for efficient use of arable land is clear, but even in regions of the world where weather and climate forecasts are most accurate, the fluctuations in rainfall and temperature that dictate the productivity of agricultural areas are largely unpredictable beyond synoptic time scales at a useful resolution.

One approach used to gain a better understanding of local land–atmosphere processes is regional modeling. Though limited in predictive ability by the use of boundary conditions and prescribed sea surface temperatures (SSTs), regional models are able to resolve important processes at sub–general circulation model (GCM) spatial scales. Regional Climate Model version 3 (RegCM3)

Corresponding author address: Jonathan M. Winter, MIT Bldg. 48-216, 15 Vassar Street, MA 02139.
E-mail: jwinter@mit.edu

DOI: 10.1175/2008JCLI2541.1

was chosen because of its proficiency in simulating energy and water dynamics throughout North America (Pal et al. 2000). Additionally, RegCM3 has been used extensively in a variety of climate studies, including an exploration of the sensitivity of regional climate to deforestation in the Amazon basin (Eltahir and Bras 1994), an investigation of the impact of tundra ecosystems on the surface energy budget and climate of Alaska (Lynch et al. 1999), and the implementation of a large-scale cloud/precipitation scheme and model verification using satellite- and station-based datasets (Pal et al. 2000). Several previous studies have employed coupled regional climate–dynamic vegetation models, including Eastman et al. (2001) and Kumar et al. (2008).

Without validation, models are of limited use. RegCM3 coupled to Integrated Biosphere Simulator (RegCM3–IBIS) and RegCM3 with its current land surface model, Biosphere–Atmosphere Transfer Scheme 1e (RegCM3–BATS1e), are evaluated against observations to gain a better understanding of the current state of surface physics modeling.

2. Model and dataset description

This section briefly describes RegCM3, IBIS, and the datasets used in the analyses.

a. RegCM3

RegCM3 is a three-dimensional, sigma-coordinate, hydrostatic, compressible, primitive-equation regional climate model that was originally developed at the National Center for Atmospheric Research (NCAR) and is currently maintained at the International Centre for Theoretical Physics (ICTP; Pal et al. 2007). RegCM3 is a descendant of the NCAR Regional Climate Model (RegCM), which was developed from the work of Dickinson et al. (1989), Giorgi and Bates (1989), and Giorgi (1990). RegCM was primarily built using the dynamical core of the fourth-generation Pennsylvania State University (PSU)–NCAR Mesoscale Model (Anthes et al. 1987).

Key components of RegCM3 include the following: the atmospheric radiation transfer computations of the NCAR Community Climate Model version 3 (CCM3; Kiehl et al. 1996); the planetary boundary layer (PBL) scheme of Holtslag et al. (1990); BATS1e for land surface processes (Dickinson et al. 1993); the ocean flux parameterization of Zeng et al. (1998); Subgrid Explicit Moisture Scheme (SUBEX), a resolvable-scale (nonconvective) cloud and precipitation formulation created by Pal et al. (2000); and three convection parameterization packages—the Emanuel (1991) scheme, the Grell (1993) scheme, and the Kuo scheme of Anthes (1977).

b. Description of surface physics models

IBIS, which was developed at the University of Wisconsin—Madison by Foley et al. (1996), is a dynamic global vegetation model (DGVM) that uses a modular, physically consistent framework to perform integrated simulations of water, energy, and carbon fluxes. A complete description of the biophysical processes contained in IBIS can be found in Pollard and Thompson (1995). IBIS includes four modules organized with respect to their temporal scale: land surface processes, soil biogeochemistry, vegetation dynamics, and vegetation phenology (Fig. 1). Based on the Land Surface Transfer Scheme (LSX) by Thompson and Pollard (1995a,b), the IBIS land surface module simulates energy, water, carbon, and momentum balances of the soil–vegetation–atmosphere system (Kucharik et al. 2000). The land surface module contains two vegetation layers, three snow layers, and up to six soil layers, allowing it to resolve changes in state variables both within the lower (shrubs, grasses) and upper (trees) canopies, as well as in each individual layer of soil and snow (Kucharik et al. 2000).

BATS1e is a comprehensive model of land surface processes that can be run offline, coupled to a GCM, or coupled to RegCM3 (Dickinson et al. 1993). BATS1e simulates a single-layer canopy with two soil layers and one snow layer. Full documentation of BATS1e can be found in Dickinson et al. (1993). BATS1e performs the following six major tasks: initializing vegetation and soil characteristics; calculating surface albedo, drag coefficient, and momentum drag; computing leaf area index (LAI), wind in the canopy, stomatal resistance, and other vegetation parameters; computing transpiration, leaf evaporation rates, dew formation, and leaf temperature; determining soil moisture, soil temperature, runoff, and snow cover; and calculating sensible and latent heat fluxes.

While the models are similar, some significant differences exist in the underlying structure, as well as at initialization.

Many differences are related to the more detailed treatment of vegetation in IBIS. Each grid cell in BATS1e has an assigned vegetation class with parameters that define the vegetation albedo, soil properties, fractional vegetation cover, roughness characteristics, etc. IBIS has a two-layer canopy in which any number of plant functional types (PFTs) may exist in each grid cell. PFTs are explicitly allowed to compete for light and water. For most calculations, including water and carbon fluxes, each PFT is treated separately and then aggregated to determine grid cell values. Canopy height and roughness parameters are variable in IBIS, but fixed in BATS1e. LAI is a function of temperature in both models, but LAI is also influenced by soil moisture in IBIS.

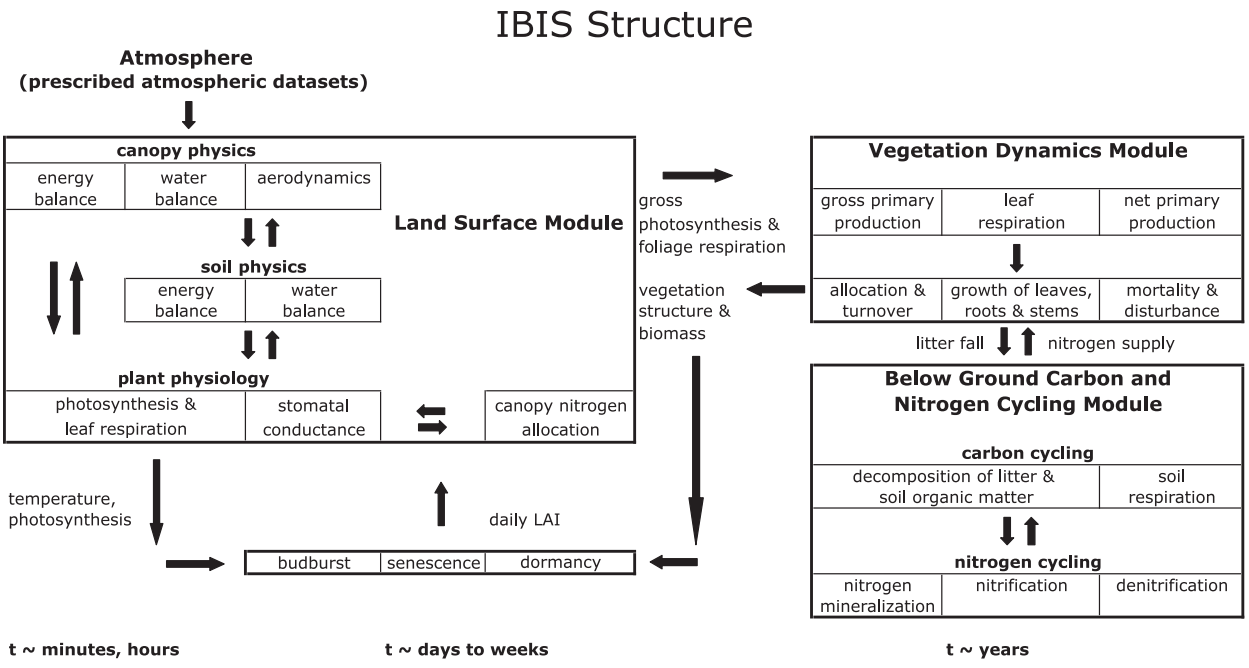

FIG. 1. Schematic of IBIS. The characteristic time scales of the processes are indicated at the bottom of the figure (Kucharik et al. 2000).

The regulation of water vapor and carbon dioxide fluxes between the vegetation and atmosphere also differs. BATS1e uses an empirical relationship between light, temperature, and water vapor pressure to determine the photosynthetic rate and stomatal resistance. Transpiration is calculated using a method similar to that of the one-layer formulation credited to Monteith (Thom and Oliver 1977), and is dependent primarily on stomatal resistance, aerodynamic resistance, and a potential evaporation rate. IBIS employs a mechanistically based approach for photosynthesis (Farquhar et al. 1980; Farquhar and Sharkey 1982) and stomatal conductance (Ball et al. 1986; Lloyd 1991; Lloyd and Farquhar 1994; Friend 1995; Leuning 1995). Photosynthesis in IBIS is a function of absorbed light, leaf temperature, CO_2 concentration in the leaf, and the Rubisco enzyme capacity for photosynthesis; stomatal conductance is dependent on photosynthetic rate, CO_2 concentration, and water vapor concentration (Foley et al. 1996). Stomatal conductance and aerodynamic conductance are combined to find a transfer coefficient, which is then used with the gradient of specific humidity between levels to find evapotranspiration.

Two key features found in IBIS that are not available in BATS1e are dynamic vegetation and an explicit carbon cycle. Summing hourly fluxes of carbon (gross photosynthetic and respiration rates) yields an annual carbon balance. Gross primary productivity and net primary productivity are calculated for each PFT. IBIS contains three basic biomass pools in which carbon may reside: leaves, woody biomass, and fine roots. Changes in each biomass pool are calculated and mortality and tissue turnover are simulated by assigning residence times to each biomass compartment. Potential LAI is calculated by dividing the carbon in the leaf biomass pool by the specific leaf area (Foley et al. 1996). When running in dynamic vegetation mode, IBIS updates the assignment of biomes annually based on the distribution of potential LAI among PFTs. For example, a grid cell in which the highest potential LAI is assigned to grasses will be designated a grassland biome, whereas an area dominated by temperate broadleaf deciduous trees will be a temperate deciduous forest biome.

In IBIS, 1 of 15 biomes is specified for each land point using a potential (undisturbed) vegetation input dataset at initialization. Then, based on climatic variables also derived from input datasets, vegetation cover for both the upper and lower canopies is assigned using a distribution of one or more of the 12 PFTs available. In RegCM3–BATS1e, vegetation classes are directly assigned using a satellite-based dataset. While this is a fundamental difference between the models that cannot be avoided, the effects of the different treatments of vegetation were minimized by choosing to examine areas that had similar vegetation cover.

Initial soil characteristics are assigned by vegetation type in RegCM3–BATS1e. For example, a desert grid point would be assigned a coarse, sandy soil with a low

soil water fraction, while for a deciduous forest, a wetter, finer soil with silt and clay would be specified. The original version of IBIS sets soil moisture to a constant for all grid cells; however, a new scheme for initializing soil moisture and temperature in RegCM3–IBIS was developed. Because IBIS is available as an offline model, which is forced using prescribed atmospheric data, it can be run for decades relatively inexpensively with respect to computational time. By modifying the offline version of IBIS, it is possible to output the soil moisture, soil ice, and soil temperature for each soil layer. This dataset can then be used in the initialization subroutine of RegCM3–IBIS, allowing for a more accurate (relative to the offline version of IBIS) initialization of soil moisture and temperature.

c. Datasets

RegCM3–IBIS and RegCM3–BATS1e were evaluated using three observational datasets; a brief description of each is provided. The Climate Research Unit (CRU) Time Series 2.0 (TS2.0) dataset contains observed surface temperature, water vapor pressure, and precipitation resampled on a 0.5° × 0.5° regular latitude–longitude grid (Mitchell et al. 2004). Some aspects of the energy budget were evaluated using the National Aeronautics and Space Administration (NASA) Surface Radiation Budget (SRB) dataset, obtained from the NASA Langley Research Center Atmospheric Science Data Center (available online at http://eosweb.larc.nasa.gov). After processing, the dataset has a 1.0° × 1.0° resolution on a regular latitude–longitude grid. FLUXNET is a network of micrometeorological tower sites that provides eddy covariance flux measurements of carbon, water vapor, and energy between the land surface and atmosphere. Currently the network includes over 400 tower sites operating both on a long-term and continuous basis (Baldocchi et al. 2001).

Three FLUXNET sites were chosen based on their proximity to agriculturally productive areas and the availability of data for the time period examined. Bondville, Illinois (40.0°N, 88.3°W), is an agricultural site with an annual rotation between soybeans (1998) and corn (1997 and 1999). The climate is temperate continental and the vegetation type is cropland. Park Falls, Wisconsin (45.9°N, 90.3°W), is situated in the Chequamegon National Forest. The vegetation cover at this site is evergreen needleleaf/temperate forest and the climate is cool continental. Little Washita Watershed (35.0°N, 98.0°W) is located near Chickasha, Oklahoma. The climate is temperate continental and the vegetation type is grassland. The FLUXNET data used in this analysis are point measurements, generally taken hourly, and are derived from the FLUXNET Marconi Conference gap-filled flux and meteorology data (Falge et al. 2005).

It is important to note that there are some errors associated with the FLUXNET observations, and that the energy budget does not close. To address this, the energy budget of the FLUXNET observations was closed using the methodology of Twine et al. (2000). Specifically, the ground heat flux was subtracted from the net radiation to find the available energy, and then the latent and sensible heat fluxes were scaled while preserving the Bowen ratio to match the available energy. At Park Falls no soil heat flux data are available. The closest proxy data for the soil heat flux at Park Falls is Willow Creek, Wisconsin. Approximately 22 km from Park Falls, the Willow Creek soil heat flux for 1999 was used for the soil heat flux at Park Falls.

3. Coupling

Building on the work of J. S. Pal (2002, personal communication) and Delire et al. (2002), IBIS was coupled to RegCM3 with one subroutine responsible for interfacing the two models, as well as additional minor changes to the RegCM3 and IBIS source codes.

The coupling of RegCM3 and IBIS involved the following five primary tasks: initialization, passing variables from RegCM3 to IBIS, passing variables from IBIS to RegCM3, restart, and output. Consideration was given to future developments of each model, and, when possible, changes to the original IBIS and RegCM3 code were avoided.

The offline version of IBIS creates its input variables from seven files containing monthly mean climatologies that are perturbed by a weather generator and used by the rest of the model. None of the datasets used by the offline version of IBIS are needed in RegCM3–IBIS except at initialization, where climatic conditions and the distribution of biomes are required for the allocation of PFTs within the domain. Instead, 12 forcing fields are passed from RegCM3 to IBIS at every time step. These variables are listed in Fig. 2. The transfer of data from IBIS to RegCM3 is handled in much the same way as the input. A list of variables passed from IBIS to RegCM3 is included in Fig. 2. The coupling time scale of RegCM3 and IBIS is a user-defined value based on the time step of the simulation.

The vegetation dataset used by the offline version of IBIS was added to the RegCM3 preprocessor, allowing IBIS biomes to be assigned during initialization. Two additional biomes, inland water and ocean, were added to the set of biomes contained in the offline version.

Another change to the preprocessing of RegCM3–IBIS is the way in which soil types are defined. Two files

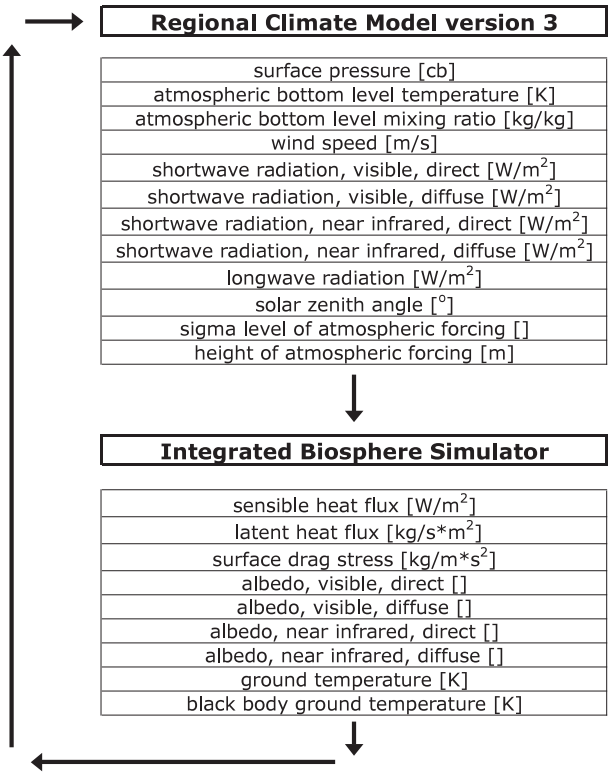

FIG. 2. Flowchart of RegCM3–IBIS, including passed variables and their associated units.

are read in, with one containing the percentage of clay and the other the percentage of sand. These data are then interpolated to the RegCM3 grid and assigned physical properties such as porosity, albedo, density, etc., based on the clay and sand fractions.

While numerical models are sometimes tuned in an attempt to match model results to observations, this was not done for any of the simulations presented. All parameters were set to the default values for both models.

4. Design of experiments

Simulations were initialized on 1 April 1995 and were allowed to spin up for 9 months. The subsequent 4 yr of simulated climate were used to evaluate the models. Centered at 40°N, 95°W, using a rotated Mercator projection, and spanning 100 points zonally and 60 points meridionally at a horizontal grid spacing of 60 km, the domain covers all of the United States, as well as parts of Mexico and Canada (Fig. 3). The years simulated (1996, 1997, 1998, and 1999) were chosen for maximum overlap with observational datasets. In all simulations presented, the surface physics scheme was run every 600 s, or once every three model time steps.

The 40-yr European Centre for Medium-Range Weather Forecasts (ECMWF) Re-Analysis (ERA-40) dataset (Uppala et al. 2005) was used to force the boundaries under the exponential relaxation of Davies and Turner (1977). SSTs were prescribed using the National Oceanic and Atmospheric Administration Optimum Interpolation SST dataset, which has a spatial resolution of 1.0° × 1.0° and is averaged on a weekly basis (Reynolds et al. 2002). This dataset relies on in situ and satellite SSTs, as well as SSTs simulated from sea ice cover (Reynolds et al. 2002). For RegCM3–IBIS, vegetation biomes were assigned using the potential global vegetation dataset of Ramankutty (1999). In addition, the following two climatology datasets were required to populate each grid cell with PFTs: the monthly mean climatology of temperature (New et al. 1999) and the minimum temperature ever recorded at a location minus the average temperature of the coldest month, created at the University of Oregon (Bartlein 2000). In all simulations presented, RegCM3–IBIS was run with static vegetation to create a consistent comparison among models. Vegetation in RegCM3–BATS1e was initialized using the Global Land Cover Characterization (GLCC) dataset of the U.S. Geological Survey (USGS; USGS 1997). The vegetation cover (biomes for RegCM3–IBIS and vegetation classes for RegCM3–BATS1e) over each point examined is provided in Table 1. Topography for both models was given by the USGS global 30-arc second elevation dataset (USGS 1996) aggregated to a 0.5° × 0.5° spatial resolution.

Because initialization of soil moisture has been shown by Fischer et al. (2007) to be important in the simulation of European heat waves, two different types of soil moisture initialization were used in RegCM3–IBIS. In the first RegCM3–IBIS simulation, soil moisture, soil temperature, and soil ice were assigned using a global 0.5° × 0.5°, 15-yr offline IBIS simulation starting in 1980. The monthly mean climatology variables required to run the offline version of IBIS are cloudiness, precipitation rate, relative humidity, temperature, ''wet'' days per month, wind speed at $\sigma = 0.995$, and temperature range, which are all products of the Climate Research Unit dataset (New et al. 1999). In the second simulation, RegCM3–IBIS with BATS1e soil moisture initialization (RegCM3–IBIS BSMI), the soil moisture and temperature fields at initialization were set identical to those of RegCM3–BATS1e. Figure 4 describes the summer seasonal cycles of surface and root zone soil moisture in RegCM3–IBIS, RegCM3–IBIS BSMI, and RegCM3–BATS1e. Surface soil moisture is presented as the soil water fraction of the surface soil layer, which is the same for both models (0–10 cm). Root zone soil moisture is the soil water fraction for the root zone soil layer, the thickness of which varies in BATS1e based on vegetation type (0–100 cm and 0–200 cm) and is fixed in IBIS (0–100 cm).

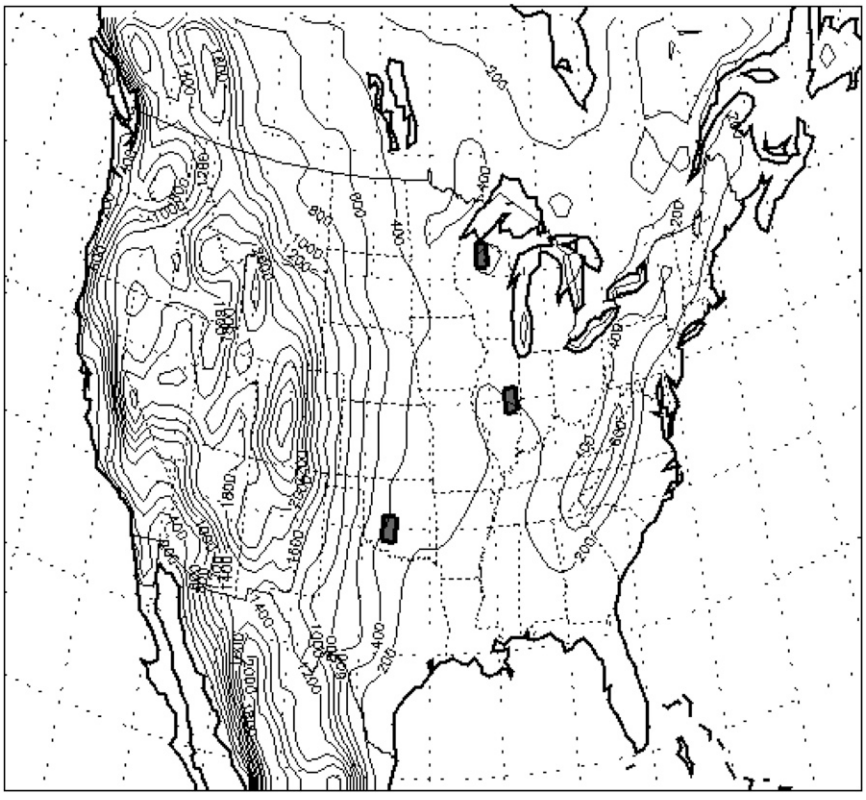

FIG. 3. Domain and topography (m) with, from north to south, 1.0° × 1.0° shaded boxes delineating the extent of spatial averaging over Park Falls, Bondville, and Little Washita Watershed.

Overall, the results of RegCM3–IBIS and RegCM3–IBIS BSMI are very similar, which suggests that for this set of experiments soil moisture initialization is not an important source of variability in the modeling results. In sections 5a and 5b, RegCM3–IBIS BSMI is discussed if its results are significantly different from RegCM3–IBIS.

Figure 5 is included to illustrate the absence of trends in surface and root zone soil moisture over the years examined.

5. Results and discussion

RegCM3–IBIS and RegCM3–BATS1e were evaluated at the three FLUXNET sites discussed above. For both models the presented results, as well as those of CRU TS2.0 and NASA SRB, are 1.0° × 1.0° spatial averages centered over the FLUXNET tower site. This resolution was chosen to maintain consistent spatial averaging among models and datasets. For reference, three 1.0° × 1.0° boxes are shown in Fig. 3, with the top box centered over Park Falls, the middle box over Bondville, and the bottom box over Little Washita Watershed. Both the Illinois and Wisconsin sites have temporal coverage for January 1997 through December 1999, while data over the Oklahoma site are only available from May 1996 to December 1998. Variables from Illinois and Oklahoma are measured at the tower top: 8 and 3 m, respectively. The FLUXNET tower in

TABLE 1. Biomes for RegCM3–IBIS and RegCM3—IBIS BSMI; and vegetation classes for RegCM3–BATS1e over the domains examined (1.0° × 1.0° boxes shown in Fig. 3). The distribution of vegetation classes within each box is given by the fraction in parentheses.

	RegCM3–IBIS/RegCM3–IBIS BSMI	RegCM3–BATS1e
Bondville	Savanna (6/6)	Cropland (5/6)
	—	Forest/field mosaic (1/6)
Park Falls	Mixed forest/woodland (6/6)	Mixed woodland (4/6)
	—	Forest/field mosaic (2/6)
Little Washita Watershed	Grassland (4/6)	Short grass (3/6)
	Savanna (2/6)	Forest/field mosaic (3/6)

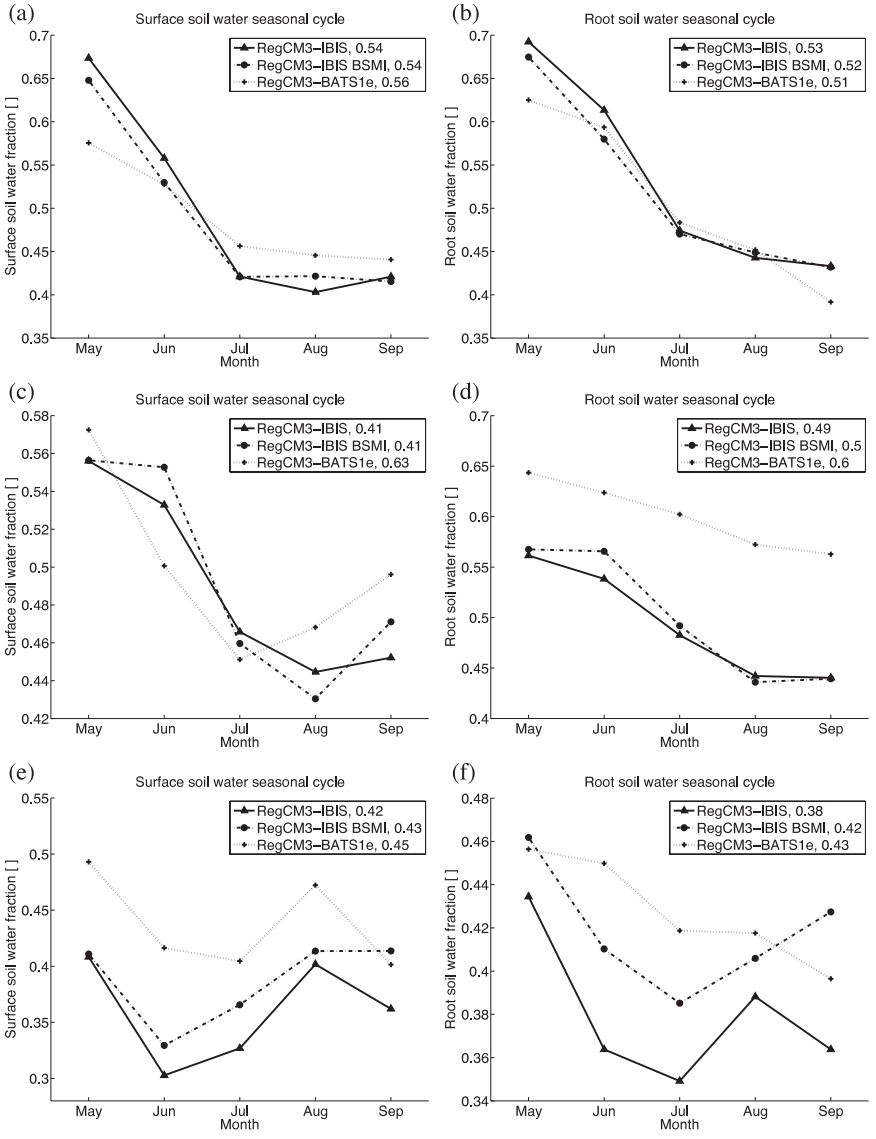

FIG. 4. Summer surface (0–10 cm) and root zone (0–100 and 200 cm) soil moisture seasonal cycles for (a), (b) Bondville, (c), (d) Park Falls, and (e), (f) Little Washita Watershed. Each value is a spatial average over a 1.0° × 1.0° box for the years of 1996–99. The 5-month average is shown in the key.

Wisconsin has instruments at 30, 122, and 396 m. Values are derived from a mix of levels, as described in Davis et al. (2003).

To evaluate the performance of the models over all seasons, the average energy budget of each is described in section 5a. The values of surface variables during the summer are especially pertinent to questions of agricultural productivity, heat waves, and soil moisture. Therefore, surface variables simulated by RegCM3–IBIS and RegCM3–BATS1e are examined for the months of June–August in section 5b. Results are summarized in section 5c. By evaluating the ability of each model to simulate the overall energy budget, and then focusing on its performance with respect to water, energy, and temperature during the summer, the general behavior and biases of RegCM3–IBIS and RegCM3–BATS1e are investigated.

a. Annual energy budget analysis

A full energy budget is provided for each site in Figs. 6–8. Shortwave radiation incident at the surface (SWI), shortwave radiation absorbed at the surface (SWN), net longwave radiation at the surface (LWN), net radiation at the surface (Rnet), latent heat flux (LH), and sensible heat flux (SH) are shown. Values for FLUXNET are point measurements averaged over the dates available, while for all other datasets values are

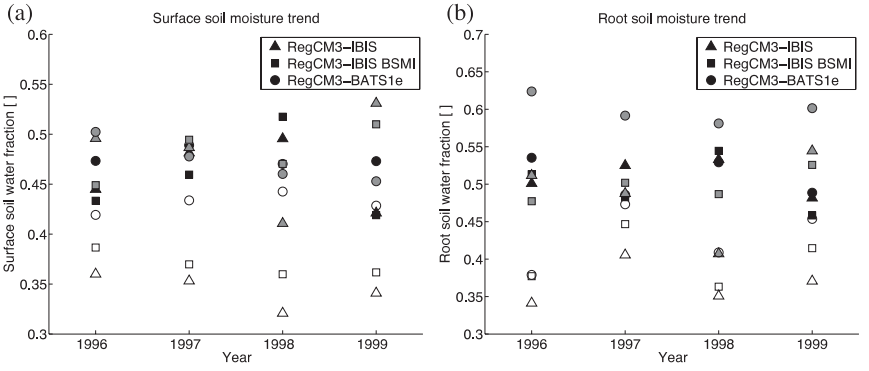

FIG. 5. 1996–99 June–August average soil moisture for Bondville (black), Park Falls (gray), and Little Washita Watershed (white).

1.0° × 1.0° spatial averages centered over the FLUXNET site and averaged over 4 yr.

Shortwave radiation incident at the surface is overestimated by RegCM3–IBIS and RegCM3–BATS1e when compared to NASA SRB at Illinois and Oklahoma. Over Wisconsin, shortwave radiation incident at the surface is correctly simulated by RegCM3–IBIS and underestimated by RegCM3–BATS1e. However, during the summer RegCM3–IBIS and RegCM3–BATS1e overestimate shortwave radiation incident at the surface for all sites. Possible causes for the overestimation of shortwave radiation incident at the surface are considered in section 5b.

RegCM3–IBIS absorbs the most shortwave radiation at the surface for all sites, a result of overestimated solar radiation incident and a lower surface albedo. RegCM3–BATS1e simulates excess shortwave radiation absorbed at the surface compared with NASA SRB for Illinois and Oklahoma, although the magnitude of the overestimation is less than that of RegCM3–IBIS. At the Wisconsin site, the amount of shortwave radiation absorbed at the surface by RegCM3–BATS1e is less than that observed, consistent with the underestimation of shortwave radiation incident at the surface.

RegCM3–IBIS overestimates net longwave radiation, a product of higher surface temperatures (discussed in section 5b) that drive increased upward longwave radiation. RegCM3–BATS1e overestimates net longwave radiation over Oklahoma, but to a lesser extent.

Net radiation values are similar for all models/datasets. Over Oklahoma and Wisconsin, NASA SRB values for net radiation are approximately 10 W m^{-2} more than RegCM3–IBIS and RegCM3–BATS1e. Over Illinois, net radiation values for RegCM3–IBIS and RegCM3–BATS1e are very similar to those of NASA SRB and are ≈10 W m^{-2} more than those of FLUXNET.

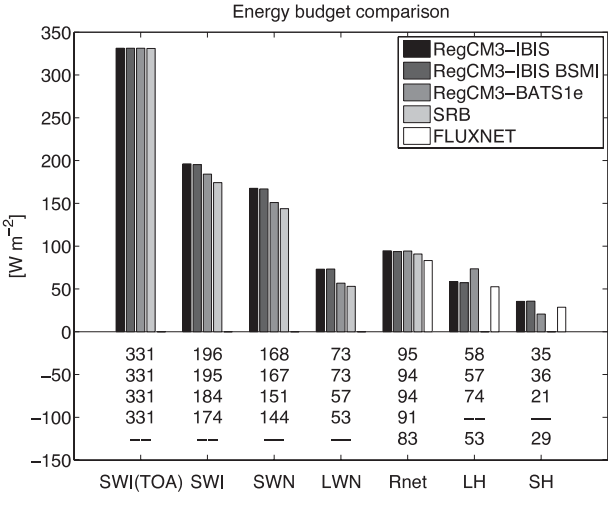

FIG. 6. Energy budget for Bondville. Each bar is a 4-yr average (1996–99) of the domain contained within the 1° × 1° box centered over Bondville, with the exception of FLUXNET, which is a point measurement averaged over the dates available.

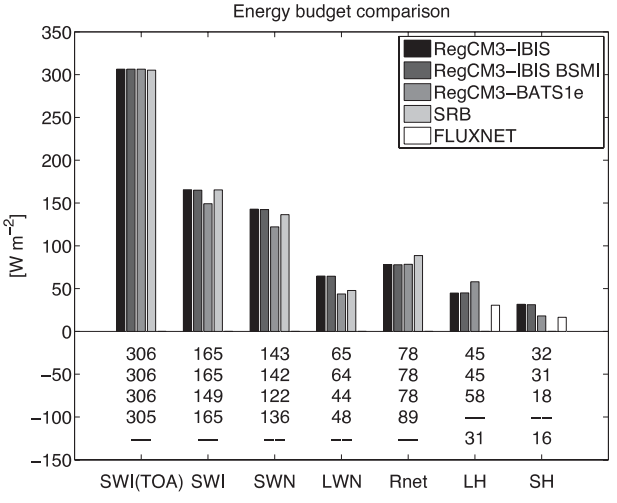

FIG. 7. Same as Fig. 6, but for Park Falls.

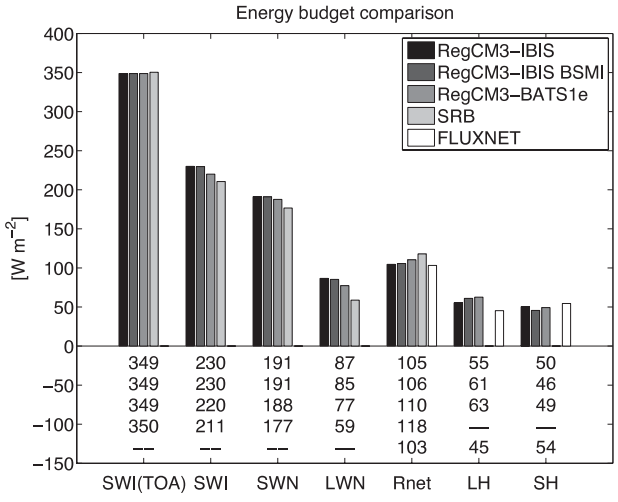

FIG. 8. Same as Fig. 6, but for Little Washita Watershed.

RegCM3–BATS1e overestimates latent heat flux at all sites. RegCM3–IBIS performs better, but still simulates excess evapotranspiration compared to FLUXNET.

RegCM3–IBIS overestimates sensible heat flux over Illinois and Wisconsin, a result of the high surface temperatures simulated by the model. RegCM3–BATS1e simulates significantly less sensible heat than RegCM3–IBIS, and agrees reasonably well with FLUXNET.

b. Summer surface variable analysis

Figure 9 shows the average June–August 2-m temperature and precipitation biases of RegCM3–IBIS and RegCM3–BATS1e when compared to CRU TS2.0 over the continental United States. RegCM3–IBIS has a large warm bias that is most intense over the midwestern United States. Temperature is significantly better simulated by RegCM3–BATS1e, although a slight warm bias is also found over the Midwest. Precipitation is overestimated by both RegCM3–IBIS and RegCM3–BATS1e; however, RegCM3–IBIS appears to have less of a wet bias. Differences between 500-mb geopotential heights and winds in RegCM3–IBIS and RegCM3–BATS1e were also examined (not pictured). No significant differences among these variables were found.

In Figs. 10–12, the following eight variables are evaluated at each site: 2-m temperature, 2-m specific humidity, latent heat flux, sensible heat flux, surface shortwave incident radiation, surface shortwave absorbed radiation, precipitation, and surface runoff. Paired in scatterplots, these components comprise four variables

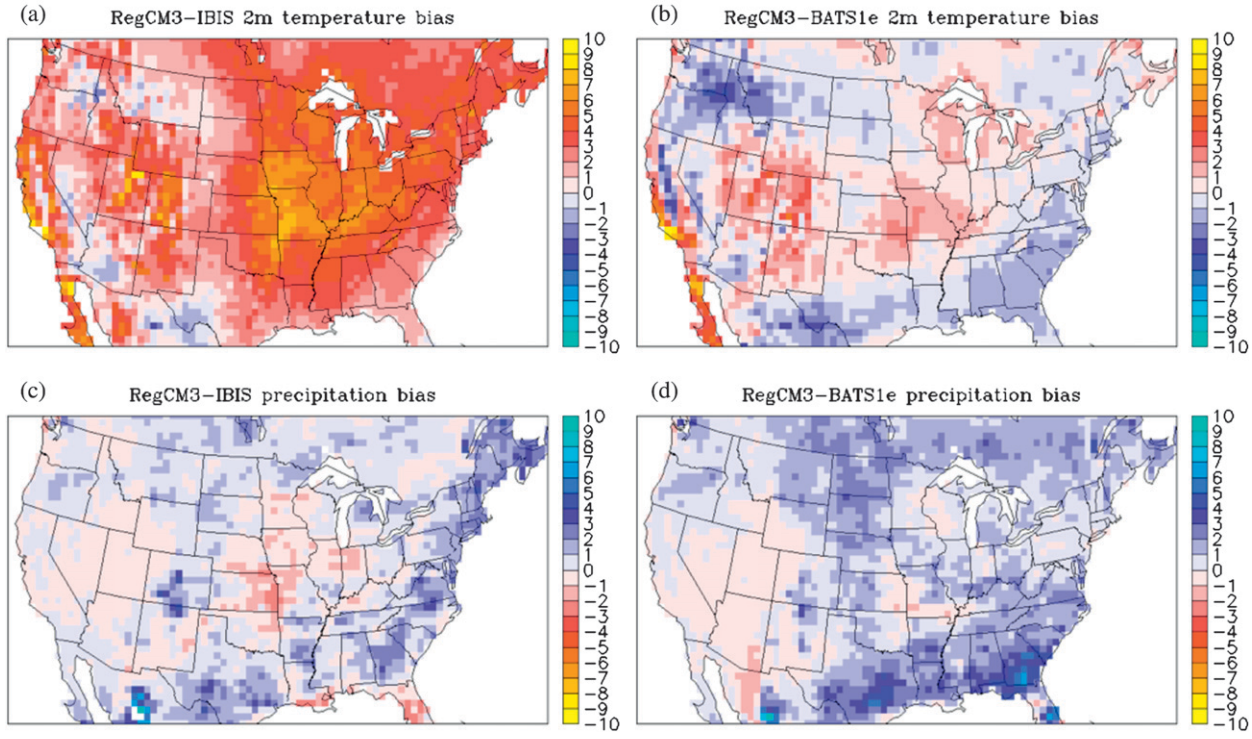

FIG. 9. Average 2-m temperature (°C) and precipitation (mm day^{-1}) biases for RegCM3–IBIS and RegCM3–BATS1e compared to CRU TS2.0 for June–August of the years of 1996–99. The bias in RegCM3–IBIS precipitation over western Mexico (three white boxes) is $\approx$ 15 mm day^{-1}.

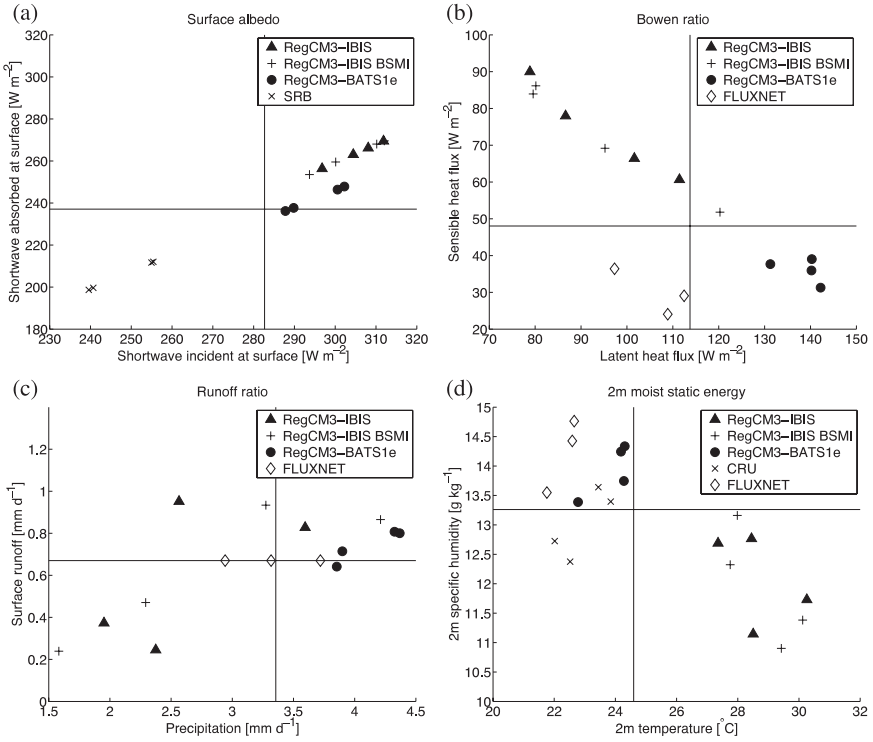

FIG. 10. Comparison of (a) surface albedo components, (b) Bowen ratio components, (c) runoff ratio components, and (d) 2-m moist static energy components for Bondville. Each point is a June–August average for 1 yr, 1996–99 (FLUXNET, dates available). FLUXNET values are point measurements, while all other values are spatial averages over a 1.0° × 1.0° box.

that are important to the performance of land surface models: the 2-m moist static energy (MSE), Bowen ratio, surface albedo, and runoff ratio. The values of these variables can be found in Table 2. Each point is a June–August average for 1 yr, and no differentiation is made between years. With the exception of FLUXNET data, which are point measurements, all presented values are 1.0° × 1.0° spatial averages. The horizontal and vertical lines are the average values over all datasets and years for variables on the y and x axes, respectively. Note that FLUXNET temperature and specific humidity are not measured at 2 m as indicated by the figure labels. The 2-m MSE is defined as

$$\mathrm{MSE} = C_p T + L_v q + gz,$$

where C_p is the specific heat of air, T is temperature, L_v is the latent heat of vaporization, q is specific humidity, and z is height (assumed to be zero in this study).

For all sites, RegCM3–IBIS absorbs the most shortwave radiation at the surface, and also receives the most incident shortwave radiation at the surface. Compared with NASA SRB, both variables are overestimated by ≈50 W m^{-2} over Illinois and Wisconsin, and ≈25 W m^{-2} over Oklahoma. RegCM3–BATS1e also overpredicts absorbed and incident shortwave radiation values, on average ≈40 W m^{-2} for the Illinois site and ≈20 W m^{-2} over Wisconsin and Oklahoma. Solar radiation at the top of the atmosphere (Figs. 6–8) is the same for both models and NASA SRB; therefore, the bias in shortwave incident radiation is primarily an atmospheric problem, likely the result of a lack of absorbed and reflected radiation in the atmospheric column. Zhang et al. (1998) concluded that the NCAR CCM3 does not absorb sufficient shortwave radiation in the atmosphere, creating an overestimation of shortwave radiation incident at the surface. Because the radiation scheme of RegCM3 is based on CCM3, it is probable that RegCM3 also suffers from the same bias. The underestimation of reflected radiation could be a result of a bias in the simulated cloud cover, an underestimation of the reflectivity of clouds that do exist, or a combination of the two. In RegCM3–IBIS, the overestimation of shortwave radiation absorbed at the surface is exacerbated by a lower surface albedo over Illinois and Wisconsin (Table 2).

RegCM3–BATS1e simulates substantially more evapotranspiration than is observed at the Illinois and Wisconsin FLUXNET sites, on average ≈40 W m^{-2}. Latent heat

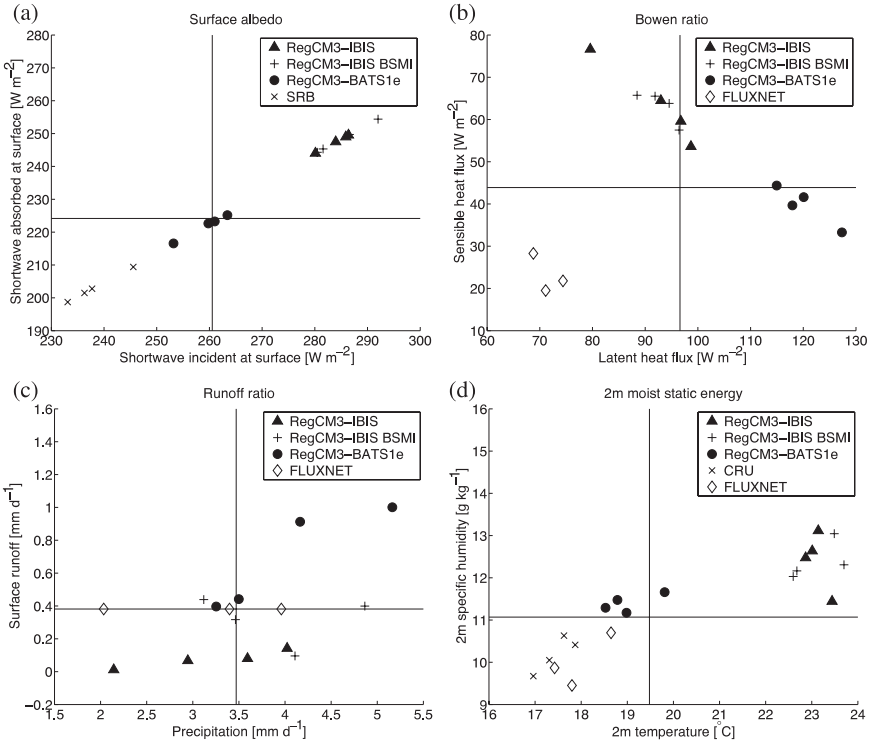

FIG. 11. Same as Fig. 10, but for Park Falls.

flux over Oklahoma is well simulated by RegCM3–BATS1e. Evapotranspiration in BATS1e is a function of potential evaporation, stomatal resistance, and aerodynamic resistance. The overestimation of both latent and sensible heat fluxes indicate that RegCM3–BATS1e likely underestimates aerodynamic resistance; however, a low stomatal resistance is also suggested, because the overestimation of latent heat flux far outpaces that of the sensible heat flux and there appears to be little or no reduction of latent heat flux during the summertime series (not shown). The latent heat flux of RegCM3–IBIS over Illinois is similar to that of the FLUXNET observations. Compared to the Wisconsin FLUXNET observations, RegCM3–IBIS overestimates latent heat flux by ≈25 W m^{-2}. Over Oklahoma the values for latent heat flux are extremely variable, but, on average, RegCM3–IBIS simulates values that are consistent with FLUXNET observations. Interestingly, over Oklahoma, RegCM3–IBIS BSMI does simulate ≈15 W m^{-2} more evapotranspiration than RegCM3–IBIS. Consistent with Fig. 4, the variability appears to be attributable to a difference in the soil moisture content between the two models. This reinforces the idea that RegCM3–IBIS has tight physiological controls on evapotranspiration. For each site, it is important to note that site-specific vegetative cover will influence FLUXNET values of latent and sensible heat considerably. FLUXNET values are point measurements over a particular vegetation cover. RegCM3–IBIS simulates only natural vegetation, and both models have a finite number of PFTs, so the vegetation contained in the 1.0° × 1.0° averaged domain may not be identical to the vegetation at the FLUXNET tower. Also, the type of cover present will influence the magnitude and distribution of evapotranspiration in time. These discrepancies are not addressed, and could contribute to some of the differences found.

RegCM3–IBIS overestimates sensible heat flux by ≈40 W m^{-2} at all sites. In RegCM3–IBIS, sensible heat flux is determined by a temperature difference between two levels and a transfer coefficient. RegCM3–IBIS overestimates surface temperature, thus increasing the difference and significantly enhancing the sensible heat flux. The sensible heat flux simulated by RegCM3–BATS1e is comparable to FLUXNET over Illinois, and is ≈20 W m^{-2} more at both the Oklahoma and Wisconsin sites. Similar to RegCM3–IBIS, the overestimation of temperature in RegCM3–BATS1e contributes to its increased sensible heat flux. In addition, as discussed above, it is likely that RegCM3–BATS1e underestimates aerodynamic resistance, which would also enhance sensible heat flux. Commensurate with the increased latent heat flux of RegCM3–IBIS BSMI when compared to RegCM3–IBIS over Oklahoma, on average RegCM3–IBIS BMSI simulates less sensible heat at this site, ≈10 W m^{-2}.

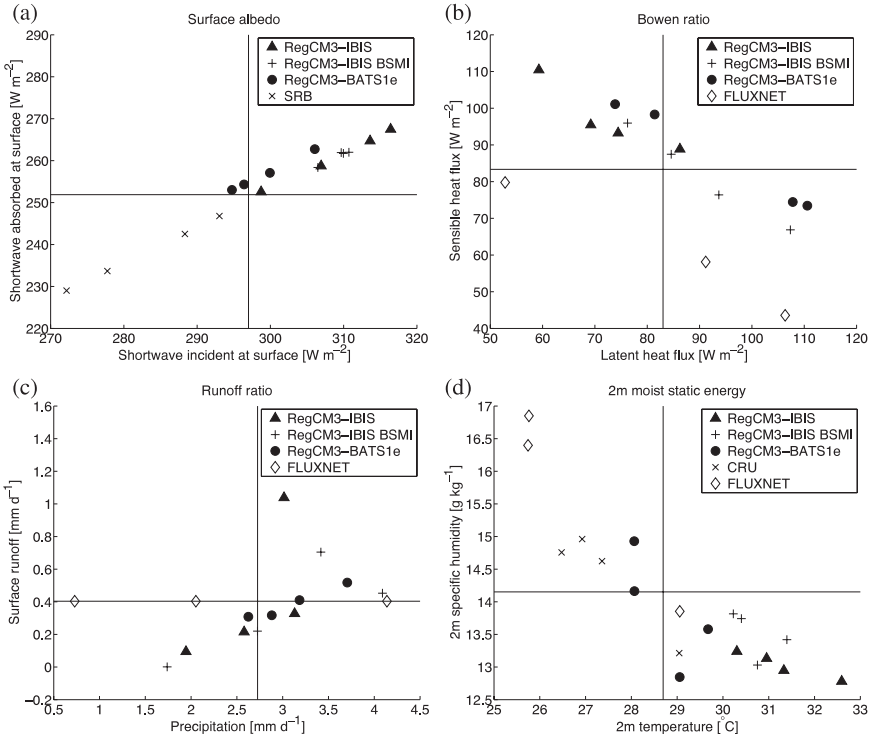

FIG. 12. Same as Fig. 10, but for Little Washita Watershed.

Precipitation values for models and observations have high interannual variability at all sites. Note that runoff values are not available for FLUXNET, so precipitation points are placed on the model/dataset average line for convenience. Few clear trends emerge. Overall RegCM3–BATS1e simulates more rainfall than RegCM3–IBIS. Consistent with the greater amount of simulated rainfall, RegCM3–BATS1e also simulates more surface runoff at all sites, and substantially more over Wisconsin. Over Illinois, RegCM3–IBIS simulates slightly less rainfall than FLUXNET, and RegCM3–BATS1e simulates slightly more. RegCM3–BATS1e overestimates rainfall at the Wisconsin site when compared to FLUXNET observations; RegCM–IBIS does not. The rainfall and surface runoff values of RegCM3–IBIS BSMI diverge from those of RegCM3–IBIS, suggesting that soil moisture initialization does play an important role in the simulation of these two variables. This is especially evident over Wisconsin, where the rainfall of RegCM3–IBIS BSMI is closer to RegCM3–BATS1e than RegCM3–IBIS.

The 2-m temperature values of CRU TS2.0 and FLUXNET generally agree for all sites. RegCM3–BATS1e does have a slight warm bias, approximately 1°C averaged across all sites. This is consistent with overestimated shortwave radiation absorbed at the surface in RegCM3–BATS1e and is likely moderated by its overestimation of latent heat flux. For each site, RegCM3–IBIS shows a clear warm bias over all of the years evaluated, on average approximately 5°C. Both excess shortwave radiation absorbed (and incident) at the surface and low latent heat fluxes drive the overestimation of temperature in RegCM3–IBIS.

RegCM3–IBIS underestimates specific humidity by $\approx$1.5 g kg^{-1} over Illinois and simulates excess specific humidity ($\approx$2 g kg^{-1}) over Wisconsin compared to FLUXNET and CRU TS2.0 observations. RegCM3–BATS1e simulates specific humidity well at all three sites. FLUXNET and CRU TS2.0 disagree significantly over Oklahoma, and both have high interannual variability.

c. *Summary*

Over the summer, RegCM3–IBIS and RegCM3–BATS1e absorb too much shortwave radiation at the surface. RegCM3–BATS1e absorbs an average of $\approx$25 W m^{-2} more shortwave radiation at the surface than NASA SRB. Faced with excess energy, the model must choose how it will balance the energy budget. In RegCM3–BATS1e, this is achieved through enhanced latent heat flux. For all sites RegCM3–BATS1e simulated more evapotranspiration than both RegCM3–IBIS and FLUXNET.

In contrast, RegCM3–IBIS has strict physiological controls on latent heat flux. This sensitivity of plants to

TABLE 2. Values for summer surface variables in Figs. 10–12. Each value is a June–August average for the years 1996–99 (FLUXNET: 1997–99 for Illinois and Wisconsin; 1996–98 for Oklahoma). FLUXNET values are point measurements, while all other values are spatial averages over a 1.0° × 1.0° box.

	Surface albedo	Bowen ratio	Runoff ratio	2m MSE (J kg^{-1})
Bondville				
RegCM3–IBIS	0.14	0.78	0.23	3.36E + 05
RegCM3–IBIS BSMI	0.14	0.78	0.22	3.35E + 05
RegCM3–BATS1e	0.18	0.26	0.18	3.35E + 05
NASA SRB	0.17	—	—	—
CRU TS2.0	—	—	—	3.32E + 05
FLUXNET	—	0.23	—	3.35E + 05
Park Falls				
RegCM3–IBIS	0.13	0.69	0.02	3.31E + 05
RegCM3–IBIS BSMI	0.13	0.68	0.08	3.31E + 05
RegCM3–BATS1e	0.14	0.33	0.17	3.24E + 05
NASA SRB	0.15	—	—	—
CRU TS2.0	—	—	—	3.20E + 05
FLUXNET	—	0.23	—	3.20E + 05
Little Washita Watershed				
RegCM3–IBIS	0.16	1.34	0.16	3.41E + 05
RegCM3–IBIS BSMI	0.16	0.90	0.12	3.41E + 05
RegCM3–BATS1e	0.14	0.93	0.13	3.40E + 05
NASA SRB	0.16	—	—	—
CRU TS2.0	—	—	—	3.40E + 05
FLUXNET	—	0.65	—	3.43E + 05

soil moisture results in smaller values of evapotranspiration, which are closer to FLUXNET observations. By not allowing the approximate 40 W m^{-2} of excess energy to leave the system as latent heat flux during the summer months, RegCM3–IBIS creates multiple other biases, all displayed in Figs. 10–12. First, the temperature of the surface increases dramatically. Second, the warming of the surface leads to increased sensible heat flux and longwave radiation upward. These primary effects cascade through the system with several possible consequences. RegCM3–IBIS will have an earlier snowmelt and therefore a lower annually averaged albedo. Evaporation from free water surfaces will increase. Given a water-limited environment, soil moisture will decrease and plants will be more likely to become water stressed, which will reduce precipitation and increase the temperature further. These results are much more dramatic than those experienced by removing excess energy as latent heat. When evapotranspiration is enhanced, the surface does not warm and the temperature may even decrease because of evaporative cooling. In this case, beside a bias in latent heat flux, no other gross observable errors exist.

6. Conclusions

The coupling of IBIS to RegCM3 is presented in this article. In addition, RegCM3–IBIS and RegCM3–BATS1e are evaluated with respect to the NASA SRB, FLUXNET, and CRU TS2.0 datasets for the period of 1996–99. Three FLUXNET sites in the midwestern United States were selected: Bondville, Illinois; Park Falls, Wisconsin; and Little Washita Watershed, Oklahoma. The skill of each model in simulating all facets of the energy budget, as well as 2-m temperature, 2-m specific humidity, precipitation, and surface runoff, was assessed at each site.

IBIS has been successfully coupled to RegCM3. The resulting model adds many features to RegCM3, including dynamic vegetation, the coexistence of multiple PFTs in the same grid cell, more sophisticated plant phenology, plant competition, explicit modeling of soil/plant biogeochemistry, and additional soil and snow layers. An improved method for initializing soil moisture and temperature has been implemented.

RegCM3–IBIS has a significant warm bias. Shortwave radiation incident, shortwave radiation absorbed, net longwave radiation, and sensible heat flux at the surface are overestimated. Latent heat flux is well simulated by RegCM3–IBIS, as is net radiation, surface runoff, and precipitation. RegCM3–BATS1e contains many of the same biases in shortwave radiation, especially during the summer months. In contrast to RegCM3–IBIS, RegCM3–BATS1e correctly simulates temperature, net longwave radiation, and sensible heat flux, but

systematically overestimates latent heat flux. RegCM3-IBIS and RegCM3-BATS1e different tendencies of models when faced with excessive radiation, a question that is particularly salient when attempting to assess the effects of changes in the radiative forcing.

To improve RegCM3–IBIS, the simulation of shortwave absorbed radiation must be corrected. This includes addressing the bias in shortwave incident radiation in the atmospheric components of RegCM3 and the underestimation of albedo in IBIS. To help correct the overestimation of surface temperature and sensible heat flux, the limitations on latent heat flux during the summer should be relaxed. Finally, anthropogenic land use biomes should be included in the model to better represent the current vegetation cover of the Midwest.

Acknowledgments. We thank the International Centre for Theoretical Physics, the Eltahir Group, members of the Ralph M. Parsons Laboratory who aided in this research, our reviewers, and our editor. Individuals who made significant contributions to this work include Filippo Giorgi and Marc Marcella. This work was funded by the National Science Foundation (Award EAR-04500341), the Linden Fellowship, and the International Centre for Theoretical Physics.

REFERENCES

Anthes, R., 1977: A cumulus parameterization scheme utilizing a one-dimensional cloud model. *Mon. Wea. Rev.,* **105,** 270–286.

——, E. Hsie, and Y.-H. Kuo, 1987: Description of the Penn State/NCAR Mesoscale Model Version 4 (MM4). NCAR Tech. Note NCAR/TN-282+STR, 79 pp.

Baldocchi, D., and Coauthors, 2001: FLUXNET: A new tool to study the temporal and spatial variability of ecosystem-scale carbon dioxide, water vapor, and energy flux densities. *Bull. Amer. Meteor. Soc.,* **82,** 2415–2434.

Ball, J., I. Woodrow, and J. Berry, 1986: A model predicting stomatal conductance and its contribution to the control of photosynthesis under different environmental conditions. *Proc. Seventh Int. Congress on Photosynthesis,* Providence, RI, 221–224.

Bartlein, P., 2000: Absolute minimum temperature minus average of the coldest monthly mean temperature Worldwide Airfield Summaries. [Available online at http://www.sage.wisc.edu/download/IBIS.]

Claassen, M. M., and R. Shaw, 1970: Water deficit effects on corn. I. Vegetative components. *Agron. J.,* **62,** 649–652.

Davies, H., and R. Turner, 1977: Updating prediction models by dynamical relaxation: An examination of the technique. *Quart. J. Roy. Meteor. Soc.,* **103,** 225–245.

Davis, K., P. Bakwin, C. Yi, B. Berger, C. Zhao, R. Teclaw, and J. Isebrands, 2003: The annual cycles of CO_2 and H_2O exchange over a northern mixed forest as observed from a very tall tower. *Global Change Biol.,* **9,** 1278–1293.

Delire, C., S. Levis, G. Bonan, J. A. Foley, M. T. Coe, and S. Vavrus, 2002: Comparison of the climate simulated by the CCM3 coupled to two different land-surface models. *Climate Dyn.,* **19,** 657–669.

Dickinson, R. E., R. M. Errico, F. Giorgi, and G. T. Bates, 1989: A regional climate model for the western United States. *Climatic Change,* **15,** 383–422.

——, A. Henderson-Sellers, and P. J. Kennedy, 1993: Biosphere Atmosphere Transfer Scheme (BATS) version 1e as coupled to the NCAR Community Climate Model. NCAR Tech. Note NCAR/TN-387+STR, 80 pp.

Eastman, J., M. Coughenour, and R. Pielke Sr., 2001: The regional effects of CO_2 and landscape change using a coupled plant and meteorological model. *Global Change Biol.,* **7,** 797–815.

Eltahir, E. A. B., and R. L. Bras, 1994: Sensitivity of regional climate to deforestation in the Amazon basin. *Adv. Water Res.,* **17,** 101–115.

Emanuel, K. A., 1991: A scheme for representing cumulus convection in large-scale models. *J. Atmos. Sci.,* **48,** 2313–2329.

Falge, E., and Coauthors, 2005: FLUXNET Marconi conference gap-filled flux and meteorology data, 1992-2000. [Available online at http://daac.ornl.gov/FLUXNET/guides/marconi_gap_filled.html.]

Farquhar, G. D., and T. D. Sharkey, 1982: Stomatal conductance and photosynthesis. *Annu. Rev. Plant Physiol.,* **33,** 317–345.

——, S. von Caemmerer, and J. A. Berry, 1980: A biogeochemical model of photo synthetic CO_2 assimilation in leaves of C_3 species. *Planta,* **149,** 78–90.

Fischer, E. M., S. I. Seneviratne, P. L. Vidale, D. Lüthi, and C. Schär, 2007: Soil moisture–atmosphere interactions during the 2003 European summer heat wave. *J. Climate,* **20,** 5081–5099.

Foley, J., I. Prentice, N. Ramankutty, S. Levis, D. Pollard, S. Sitch, and A. Haxeltine, 1996: An integrated biosphere model of land surface processes, terrestrial carbon balance, and vegetation dynamics. *Global Biogeochem. Cycles,* **10,** 603–628.

Friend, A., 1995: PGEN: An integrated model of leaf photosynthesis, transpiration, and conductance. *Ecol. Modell.,* **77,** 233–255.

Giorgi, F., 1990: Simulation of regional climate using a limited area model nested in a general circulation model. *J. Climate,* **3,** 941–963.

——, and G. Bates, 1989: The climatological skill of a regional model over complex terrain. *Mon. Wea. Rev.,* **117,** 2325–2347.

Grell, G. A., 1993: Prognostic evaluation of assumptions used by cumulus parameterizations. *Mon. Wea. Rev.,* **121,** 764–787.

Holtslag, A. A. M., E. I. F. de Bruijn, and H.-L. Pan, 1990: A high resolution air mass transformation model for short-range weather forecasting. *Mon. Wea. Rev.,* **118,** 1561–1575.

Kiehl, J. T., J. J. Hack, G. B. Bonan, B. A. Boville, B. P. Breigleb, D. L. Williamson, and P. J. Rasch, 1996: Description of the NCAR Community Climate Model (CCM3). NCAR Tech. Note NCAR/TN-420+STR, 159 pp.

King, S. S., 1981: Down on the farm, higher prices. *New York Times,* 11 January, Section 12, 01.

Kumar, S. V., C. D. Peters-Lidard, J. L. Eastman, and W.-K. Tao, 2008: An integrated high-resolution hydrometeorological modeling testbed using LIS and WRF. *Environ. Modell. Software,* **23,** 169–181.

Leuning, R., 1995: A critical appraisal of a combined stomatal-photosynthesis model for C_3 plants. *Plant Cell Environ.,* **18,** 339–355.

Lloyd, J., 1991: Modelling stomatal responses to environment in *Macadamia integrifolia*. *Aust. J. Plant Physiol.,* **18,** 649–660.

——, and G. Farquhar, 1994: ^{13}C discrimination during CO_2 assimilation by the terrestrial biosphere. *Oecologia,* **99,** 201–215.

Lynch, A. H., W. Wu, G. Bonan, and F. Chapin III, 1999: The impact of tundra ecosystems on the surface energy budget and climate of Alaska. *J. Geophys. Res.,* **104,** 6647–6660.

Mitchell, T. D., T. R. Carter, P. D. Jones, M. Hulme, and M. New, 2004: A comprehensive set of high-resolution grids of monthly climate for Europe and the globe: The observed record (1901–2000) and 16 scenarios (2001–2100). Tyndall Centre for Climate Change Research Working Paper 30. [Available online at http://www.tyndall.ac.uk/publications/working_papers/wp55.pdf.]

New, M., M. Hulme, and P. Jones, 1999: Representing twentieth-century space–time climate variability. Part I: Development of a 1961–90 mean monthly terrestrial climatology. *J. Climate,* **12,** 829–856.

Pal, J. S., E. E. Small, and E. A. B. Eltahir, 2000: Simulation of regional-scale water and energy budgets: Representation of subgrid cloud and precipitation processes within RegCM. *J. Geophys. Res.,* **105,** 29 579–29 594.

——, and Coauthors, 2007: Regional climate modeling for the developing world: The ICTP RegCM3 and RegCNET. *Bull. Amer. Meteor. Soc.,* **88,** 1395–1409.

Pollard, D., and S. L. Thompson, 1995: Use of a land-surface-transfer scheme (LSX) in a global climate model: The response to doubling stomatal resistance. *Global Planet. Change,* **10,** 129–161.

Ramankutty, N., 1999: Estimating historical changes in land cover: North American croplands from 1850 to 1992. *Global Ecol. Biogeogr.,* **8,** 381–396.

Reynolds, R. W., N. A. Rayner, T. M. Smith, D. C. Stokes, and W. Wang, 2002: An improved in situ and satellite SST analysis for climate. *J. Climate,* **15,** 1609–1625.

Thom, A. S., and H. R. Oliver, 1977: On Penman's equation for estimating regional evaporation. *Quart. J. Roy. Meteor. Soc.,* **103,** 345–357.

Thompson, S. L., and D. Pollard, 1995a: A global climate model (GENESIS) with a land-surface transfer scheme (LSX). Part I: Present climate simulation. *J. Climate,* **8,** 732–761.

——, and ——, 1995b: A global climate model (GENESIS) with a land-surface transfer scheme (LSX). Part II: CO_2 sensitivity. *J. Climate,* **8,** 1104–1121.

Twine, T. E., and Coauthors, 2000: Correcting eddy-covariance flux underestimates over a grassland. *Agric. For. Meteor.,* **103,** 279–300.

Uppala, S. M., and Coauthors, 2005: The ERA-40 Re-Analysis. *Quart. J. Roy. Meteor. Soc.,* **131,** 2961–3012.

USGS, cited 1996: Global 30-arc second elevation dataset (GTOPO30). [Available online at http://edc.usgs.gov/products/elevation/gtopo30/gtopo30.html.]

——, cited 1997: Global land cover characterization. [Available online at http://edc2.usgs.gov/glcc/.]

Zeng, X., M. Zhao, and R. E. Dickinson, 1998: Intercomparison of bulk aerodynamic algorithms for the computation of sea surface fluxes using TOGA COARE and TAO data. *J. Climate,* **11,** 2628–2644.

Zhang, M. H., W. Y. Lin, and J. T. Kiehl, 1998: Bias of atmospheric shortwave absorption in the NCAR Community Climate Models 2 and 3: Comparison with monthly ERBE/GEBA measurements. *J. Geophys. Res.,* **103,** 8919–8925.